PROCEEDINGS OF SPIE

SPIEDigitalLibrary.org/conference-proceedings-of-spie

Status of the mid-infrared E-ELT imager and spectrograph METIS

Bernhard R. Brandl, Tibor Agócs, Gabby Aitink-Kroes, Thomas Bertram, Felix Bettonvil, et al.

Bernhard R. Brandl, Tibor Agócs, Gabby Aitink-Kroes, Thomas Bertram, Felix Bettonvil, Roy van Boekel, Olivier Boulade, Markus Feldt, Alistair Glasse, Adrian Glauser, Manuel Güdel, Norma Hurtado, Rieks Jager, Matthew A. Kenworthy, Michael Mach, Jeff Meisner, Michael Meyer, Eric Pantin, Sascha Quanz, Hans Martin Schmid, Remko Stuik, Auke Veninga, Christoffel Waelkens, "Status of the mid-infrared E-ELT imager and spectrograph METIS," Proc. SPIE 9908, Ground-based and Airborne Instrumentation for Astronomy VI, 990820 (9 August 2016); doi: 10.1117/12.2233974

SPIE.

Event: SPIE Astronomical Telescopes + Instrumentation, 2016, Edinburgh, United Kingdom

Status of the mid-infrared E-ELT imager and spectrograph METIS

Bernhard R. Brandl[*a,b], Tibor Agócs[c], Gabby Aitink-Kroes[c], Thomas Bertram[d], Felix Bettonvil[a], Roy van Boekel[d], Olivier Boulade[e], Markus Feldt[e], Alistair Glasse[f], Adrian Glauser[i], Manuel Guedel[g], Norma Hurtado[c], Rieks Jager[c], Matthew A. Kenworthy[a], Michael Mach[g], Jeff Meisner[a], Michael Meyer[i], Eric Pantin[e], Sascha Quanz[i], Hans Martin Schmid[i], Remko Stuik[a,c], Auke Veninga[c], Christoffel Waelkens[j]

[a]Leiden Observatory, Leiden University, P.O. Box 9513, 2300 RA Leiden, The Netherlands;
[b]Faculty of Aerospace Engineering, Delft University of Technology, Kluyverweg 1, 2629 HS Delft, The Netherlands;
[c]NOVA O/IR Group, P.O. Box 2, 7990 AA Dwingeloo, The Netherlands;
[d]Max-Planck-Institut für Astronomie, Königstuhl 17, 69117 Heidelberg, Germany;
[e]Commissariat à l'Energie Atomique, Institut de Recherche sur les Lois Fondamentales de l'Univers, Service d'Astrophysique, Orme des Merisiers, 91191 Gif sur Yvette, France;
[f]UK Astronomy Technology Centre, Edinburgh EH9 3HJ, UK;
[g]University of Vienna, Department of Astrophysics, Türkenschanzstrasse 17, A-1180 Vienna, Austria;
[i]ETH Zürich; Institute for Astronomy, Wolfgang-Pauli-Strasse 27, CH-8093 Zürich, Switzerland;
[j]Instituut voor Sterrenkunde, K.U.Leuven, Celestijnenlaan 200D, B-3001 Leuven, Belgium.

ABSTRACT

METIS is one the first three instruments on the E-ELT. Apart from diffraction limited imaging, METIS will provide coronagraphy and medium resolution slit spectroscopy over the 3 – 19μm range, as well as high resolution (R ~ 100,000) integral field spectroscopy from 2.9 – 5.3μm, including a mode with extended instantaneous wavelength coverage. The unique combination of these observing capabilities, makes METIS the ideal instrument for the study of circumstellar disks and exoplanets, among many other science areas. In this paper we provide an update of the relevant science drivers, the METIS observing modes, the status of the simulator and the data analysis. We discuss the preliminary design of the optical system, which is driven by the need to calibrate observations at thermal IR wavelengths on a six-mirror ELT. We present the expected adaptive optics performance and the measures taken to enable high contrast imaging. We describe the opto-mechanical system, the location of METIS on the Nasmyth instrument platform, and conclude with an update on critical subsystem components, such as the immersed grating and the focal plane detectors. In summary, the work on METIS has taken off well and is on track for first light in 2025.

Keywords: METIS, E-ELT, mid-infrared, cryogenic, preliminary design, science, calibration, adaptive optics

1. INTRODUCTION

The 'Mid-infrared ELT Imager and Spectrograph' (METIS) will be one of the first three science instruments on the European Extremely Large Telescope (E-ELT). After signing the contract on the design and construction of METIS with ESO on September 28th, 2015, METIS is now in the preliminary design phase toward first light at the telescope in early 2025. The METIS consortium members are NOVA (The Netherlands, PI: Bernhard Brandl), MPIA Heidelberg (Germany), CEA-Saclay (France), UK-ATC (United Kingdom), KU Leuven (Belgium), ETH Zürich (Switzerland), and the A* Consortium (Austria).

*brandl@strw.leidenuniv.nl; phone +31 71 527 5830

Ground-based and Airborne Instrumentation for Astronomy VI, edited by Christopher J. Evans, Luc Simard, Hideki Takami
Proc. of SPIE Vol. 9908, 990820 · © 2016 SPIE · CCC code: 0277-786X/16/$18 · doi: 10.1117/12.2233974

METIS will cover the thermal/mid-infrared wavelength range (3 – 19μm), focusing on highest angular resolution and high spectral resolution, complementing ALMA and JWST. According to the agreed technical specifications, METIS will provide the following observing modes (see also section 2.3):

- Imaging at L/M (2.9 – 5.3μm) band. The imager shall include low/medium resolution (R ~ few hundred - thousands) slit spectroscopy as well as coronagraphy for high contrast imaging.
- Imaging at N/Q (7.0 – 19.0μm) band. The imager shall include low/medium resolution (R ~ few hundred - thousands) slit spectroscopy as well as coronagraphy at N-band for high contrast imaging.
- High resolution (R ~ 100,000) IFU spectroscopy at L/M band, including a mode with extended instantaneous wavelength coverage.

Focusing mostly on known, compact targets, METIS requires only a moderate (~ 10″×10″) imaging field of view size. The IFS field of view is ~ 0.5″×0.5″. All observing modes work at the diffraction limit. The atmospheric turbulence will be corrected by a single conjugate adaptive optics (SCAO) system with the option for a later upgrade to a laser tomography adaptive optics (LTAO) system.

Since this paper represents a snapshot of the design progress taken during the preliminary design phase, *all technical information presented in this paper must be considered preliminary and is subject to change*.

2. SCIENTIFIC PERFORMANCE

2.1 Science case

Given its unique capabilities in terms of spatial resolution and also spectral resolution, provided by a 39m ELT, the science case for METIS is broad and covers various science themes. These themes include the formation history of our Solar system, massive stars and cluster formation, evolved stars and their circumstellar environment, the Galactic Center, and extragalactic science, e.g., starbursts in the local Universe, luminous star-forming galaxies at high redshift, and active galactic nuclei (AGN). Two science themes, however, drive the instrument requirements, and these are (1) protoplanetary disks and the formation of planets, and (2) detection and characterization of exoplanets. Given the general scope of this paper the following subsections will focus on (1) and (2) to provide a brief illustration of the scientific capabilities of METIS.

Protoplanetary disks and the formation of planets

Leveraging METIS' high spatial resolution a key science objective is to observe, and image, the process of planet formation in the primary planet-forming regions from 1-10 AU at all evolutionary stages from protoplanetary disks through debris disks. Specifically, METIS will have the potential to transform our understanding in five areas:

- Observe the physical evolution of planet-forming material. This includes imaging the distribution of small grains (a few microns in size) for direct comparison with large grains (millimetre to centimetre) observed by ALMA, measuring the gas kinematics and amount of warm molecular gas at 1AU scales in disks, and quantifying molecular disk winds that affect disk dissipation.
- Search for proto-planets embedded in gas-rich disks, either directly or through their kinematics reflecting dynamical interactions with gas and dust. This includes a search for molecular and atomic emission from circum-planetary disks around Jupiter-mass proto-planets. The physical properties of proto-planets can be directly compared to exoplanet demographics.
- Measure the chemical composition of planet-forming gas and dust inside of 10 AU. This includes measuring the composition and distribution of warm molecular gas and PAHs in the innermost disk, observations of ices in scattered light and absorption, and the crystallinity and composition of small dust grains on 1-10 AU scales.
- Image warm dust belts in nearby debris disks to determine their properties and radial distribution. This may reveal ongoing terrestrial planet formation and constrain models of the Earth's origin.
- Search for and image exo-zodiacal systems around nearby main-sequence stars to determine their demographics in comparison to those of exoplanets.

In Figure 1 we show an example how METIS will be able to spatially resolve the kinematics of molecular gas in planet-forming regions around young, disk-bearing stars. While dust observations are critical for our understanding of planet formation, the gas component plays a comparable and complementary role and does not only drive dust dynamics, but also provides the necessary ingredient for giant planet formation. In comparison to ALMA, METIS will produce full-aperture images of *warm* molecular gas in protoplanetary disks at angular scales of 0.05″, with high efficiency and sensitivity, allowing for direct imaging of large samples of disks. In particular, the CO v=1-0 ro-vibrational transitions at 4.7 μm are excellent tracers of the 1 – 10 AU region in proto-planetary disks (e.g., [1]) probing gas with temperatures of a few hundred Kelvin to about 1000 K.

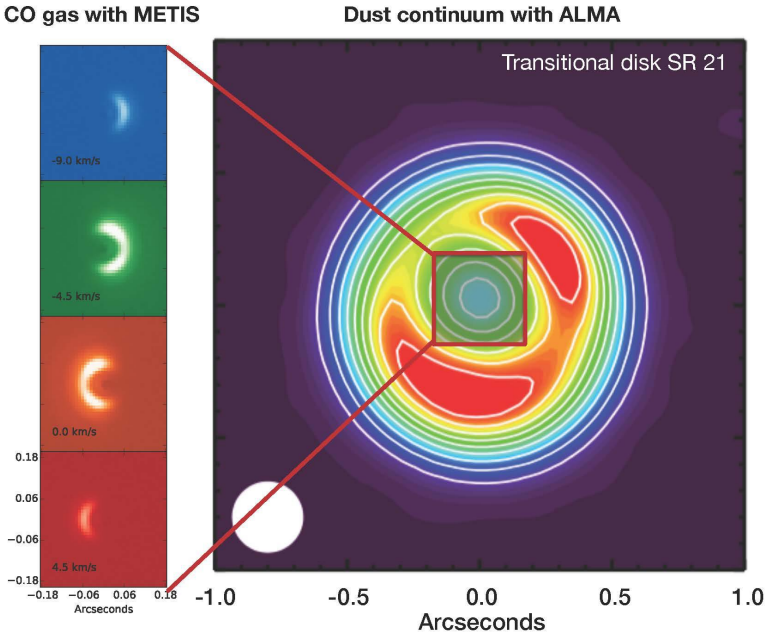

Figure 1 Model of a METIS observation of CO ro-vibrational emission at 4.7 μm in the transitional disk around SR 21, a G3 star at a distance of ≈120 pc in the Ophiuchus star-forming region. (left panels), compared to the ALMA dust continuum (0.87 mm) image (right panel; based on data presented in [2]). It is already known from CRIRES spectro-astrometric observations [3] that the CO gas traces an inner ring at ≈7 AU (corresponding to orbital separations between Jupiter and Saturn in the Solar system), separate from the outer dust ring at ≈35 AU as seen with ALMA. METIS can directly image this inner ring and provide further constraints on embedded planets shepherding the rings. The CO images represent a two-dimensional, non-LTE model with gas/dust thermal decoupling, using the radiative transfer codes RADLite/RADMC.

Exoplanet detection and characterization

The study of extrasolar planets will be one of the prime science goals and METIS will have a ground-breaking impact in both areas the detection and also the characterization of extrasolar planets. The exoplanet science case is divided into the following three main topics:

- *Exoplanet demographics*: This includes the detection of (gas giant) planets with an empirically determined mass, either from ongoing radial velocity campaigns or from ESA's GAIA mission, and also the determination of the occurrence rate of gas giant planets at large orbital separations (5-30 AU). At this point in time, none of the directly imaged planets has an empirically determined mass, and current exoplanet imaging surveys have insufficient spatial resolution and sensitivity to probe a large number of stars for planets with masses and separations comparable to the gas and ice giants in our solar system.
- *Climates and atmospheric characterization*: This topic includes both the study and characterization of close-in transiting and non-transiting planets (e.g.,[4]) and also distant cool giant planets. By tracing thermal emission from exoplanets in the mid-infrared, opacities of absorbers (molecular bands, dust, clouds), vertical temperature profiles,

and the chemical composition of exoplanet atmospheres can be constrained. Thanks to its long-slit spectroscopy and high-dispersion IFU mode, METIS will not only be able to characterize the composition and key physical parameters of exoplanet atmospheres, but it will also be capable of tracing atmospheric dynamics and exoplanets rotation rates (e.g.,[5]).

- *Towards other Earths*: The Kepler mission revealed that small planets with radii < 4 R_{Earth} are abundant (e.g.,[6]) suggesting that small planets also orbit other stars in the immediate Solar neighborhood. Theoretically, small, warm planets around the nearest stars emit enough thermal radiation for METIS to detect them and, given that at the moment no space-based missions to image Earth-like planets are on the roadmap of any space agency, significant efforts are invested to enable this science case.

Figure 2 illustrates the last topic mentioned above. More details on exoplanet science with METIS can be found in [7]. In that context, METIS offers an interesting, additional possibility: Time differential, high-dispersion spectroscopy has already shown to be able to separate out planet signals in the time and spectral domain at the 10^{-4} level. Furthermore, high-contrast direct imaging spatially separates the planets at even higher contrast levels. Simulations show that the METIS IFU (e.g., in the wavelength range from 4.8 – 4.9 μm) can combine these techniques and detect and characterize planets simultaneously in the time, spectral and spatial domain — reaching contrast levels of 10^{-9} or better — bringing even the characterization of rocky planets around nearby stars within reach [8].

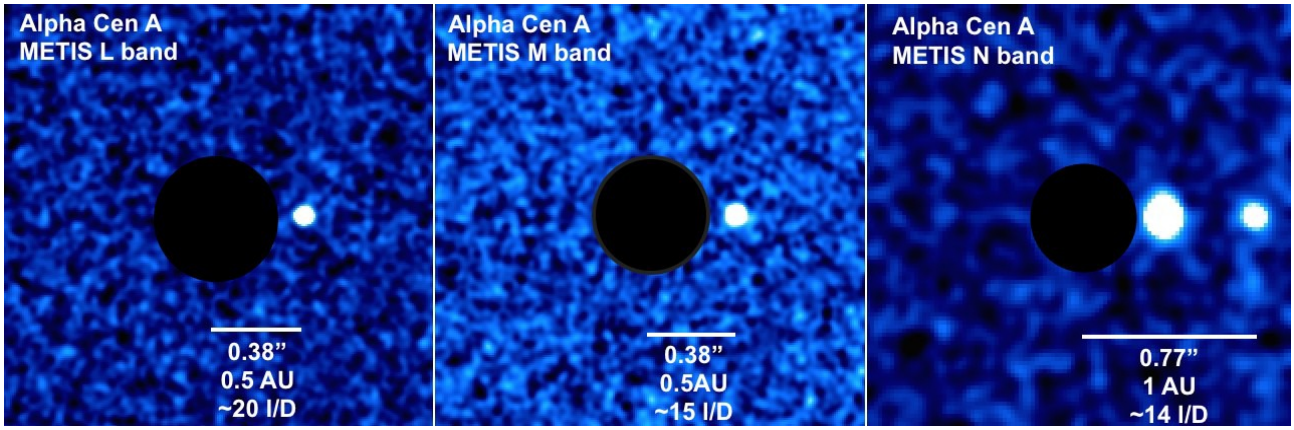

Figure 2 METIS simulations of small planets around Alpha Cen A. From left to right: 2h on source integration in the L, M and N band, respectively. The central star has been masked out in all images. Each image contains 2 planets with a radius of 1 R_{Earth}, one planet located at 0.5 AU, the other one located at 1 AU (the corresponding separation in units of λ/D is given in the different panels). Assuming a bond albedo of 0.3 for the planets and a luminosity of L=1.52 L_{Sun} for Alpha Cen A, the planets have equilibrium temperatures of ≈400 K and ≈280 K, respectively. While the inner planet is clearly detected in all METIS filters, the planet at 1 AU is only detected at N band. All simulations assume that at the location of the planets METIS is background noise limited. The contrast of the inner planet relative to the central star is $3{\cdot}10^{-9}$, $2{\cdot}10^{-8}$, and $5{\cdot}10^{-7}$, in the L, M and N band, respectively. The outer planet has a contrast of 10^{-7} in the N band.

2.2 Instrument simulator

The feasibility of the METIS science case has been tested with the METIS simulator [9]. The simulator is an evolving software tool that produces simulated detector output expected from the instrument given the most up-to-date models available. The light from an assumed astronomical object is simulated as it encounters the atmosphere, the ELT optics, and the entire chain of optical components in METIS, including the detectors from which expected readouts are generated. The simulator performs four important roles in the development and eventual use of the instrument:

- The *evaluation and preparation of science observations* and programs (in this context often referred to as an exposure time calculator) [10].

- A model implemented in software will be of value in the evaluation, testing, and development of calibration strategies [11]. This includes in particular *background subtraction through chopping* which is implemented not by the E-ELT itself but internally in METIS.
- Simulations can be run to evaluate the effects of *hardware choices* and obtain *sensitivity estimates* and other technical specifications as a function of instrument configuration.
- The *development of data reduction* components and the ESO pipeline for METIS will require use of *simulated raw data* for testing of such software, both in regards to technical programming considerations and methods used for interpretation and calibration of instrumental outputs.

Not intending to reflect the program structure itself, Figure 3 illustrates the effective processing of input data using the instrumental model. This involves tracing three aspects of the light starting from a supplied model of the underlying astronomical object up to and including the photodetectors whose simulated output frames are written into FITS files. The *image track* propagates and modifies one or more raster image planes (depending on the color-complexity of the model) with respect to spatial features. The *spectral track* processes a spectrum for each image plane, taking into account at each stage the spectral throughput of various optical elements (including the atmosphere). Finally, *the background track* models thermal emission from each such element with non-zero emissivity (optical transmission less than unity) and a specified temperature. The three tracks are combined to produce a flattened image representing detector photocurrent, to which detection noise is added and other detector effects applied. The individual raw detector outputs are available directly, but as a convenience the simulator includes basic capabilities for the summation of raw images and background subtraction that would typically be undertaken using such a sequence of detector frames.

Predicted point- and extended-source sensitivities for METIS on the E-ELT are given in [9].

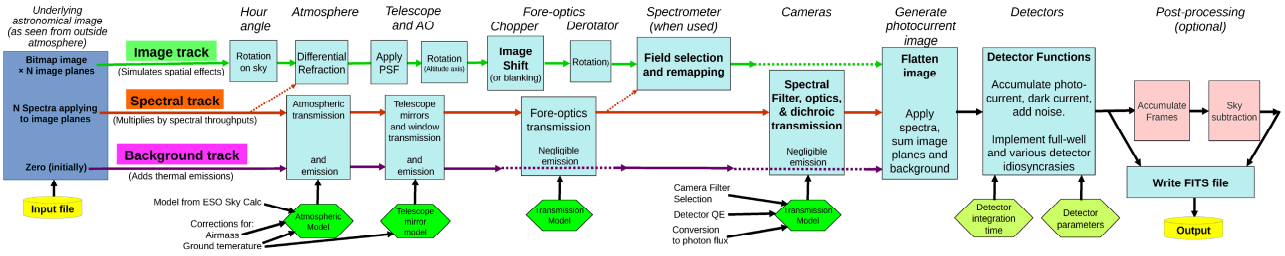

Figure 3 Simplified signal flow diagram of the METIS Simulator

2.3 Operation modes

At the most basic level METIS consists of two sub-systems (see section 3.1): an imager (IMG) and a high-resolution integral field spectrograph (IFS). The imager is subdivided into a short (LM) and long (NQ) wavelength camera. The basic observing modes reflect this architecture.

The imager can perform plain imaging through a set of broad- and narrow-band filters in each of its arms. Observations in the NQ camera will employ chopping, while chopping is optional for observations with the LM camera. Nodding/dithering will likely be employed in both cases. Each arm has a set of grisms allowing longslit spectroscopy. The LM arm has two grisms with which the entire atmospheric L- or M-band spectrum can be projected onto the detector at once at a spectral resolution of R_L ~1500 and R_M ~ 2000, respectively. The NQ arm has a grism with which the entire N-band spectrum can be recorded at R_N ~ 440. Furthermore, it is foreseen to have two medium-resolution grisms with which the spectral regions around the [SIV]10.51µm and the [NeII]12.81µm lines can be observed at a spectral resolution of R ~ 6000.

The IFS operates in the L- and M-bands, and – in its nominal mode – allows to observe 40 to 80 nm wide passbands at a spectral resolution of R = 100,000 at 4.65µm, with a rectangular field covering at least 0.5″ × 0.5″. The focal plane sampling at the image slicer is 0.5 and 1.0 times the FWHM of the diffraction-limited PSF at 3.0µm. The different wavelength ranges can be selected using appropriate settings of the pre-dispersion prism and main dispersion grating. An

extended wavelength coverage mode will be available, allowing to instantaneously observe a 5× larger spectral range at the expense of only ~1/5th of the spatial coverage of the nominal mode. It is foreseen that IFS observations are always accompanied by parallel LM imaging of the field surrounding the IFU pick-off to allow for accurate astrometric calibration of the IFS data.

METIS will also offer coronagraph-assisted observations (see section 3.2) in most of the basic modes described above. The possibility of performing Sparse Aperture Masking (SAM) observations by including corresponding pupil plane masks in the IMG is being investigated. Figure 4 gives an overview of the observing modes of METIS.

main mode	sub mode	waveband / *R* / Δλ
Imaging	direct	LMNQ
	coronagraphy	LMN
	SAM	LMNQ
spectroscopy	longslit	LM, *R*~2000
	longslit	N, *R*~440
	longslit	N, *R*~6000; ([SIV], [NeII])
	IFS nominal	LM, R=100.000, Δλ~50 nm
	IFS ext. λ	LM, R=100.000, Δλ~300 nm
	coronagraphy	LM, R=100.000, Δλ~50/300 nm

Figure 4 METIS observing modes.

2.4 Data analysis

Modern astronomical instruments produce data, which consist of a multitude of scientific and calibration frames. These data need to be combined in an often non-trivial way for data reduction. A number of software tools, called recipes in the ESO data flow system, need to be executed consecutively in a complex workflow that needs to be configured and supervised. Automation of execution of these workflows provide a gain in efficiency. The data reduction pipeline for METIS has to provide fast and reliable processing of data in large quantities with maximum data rates of up to 6 terabyte per 10 hours of observation. The detectors need to have read out rates of 20 frames per second to prevent detector saturation from the thermal background radiation. The optimum calibration strategy for subtraction of this thermal background radiation is currently being worked on, and will be incorporated into the data reduction pipeline once available. The data products of the data reduction pipeline consist of science data products, including associated error maps, master calibration frames, quality control parameters, and bad pixel masks.

Data Flow System

The design of the data reduction pipeline has to comply with ESO's data flow system (DFS), and the code for recipes has to be written using ESO's Common Pipeline Library (CPL) [12] and the upcoming High Level Data Reduction Library (HDRL). The science grade pipeline has to be provided as a REFLEX workflow [13]. The pipeline has to have three different levels of data processing to obey to ESO's standards for the data flow system:

1. *Observatory Pipeline*: for event driven, on-the-fly data processing without any user interaction.
2. *Quality Control (QC)Pipeline*: provides master calibration frames, QC parameters, quantifies data to check for system health.
3. *Science Grade Pipeline*: enables the science community to reprocess all data reduction steps individually with user defined parameters and with the best available calibration data.

The data flow of one observation block (OB) within the pipeline levels is controlled by the data organizer (DO). The DO selects all corresponding data necessary for the data reduction of one OB template. A set of rules, called "OCA (Organization, Classification, Association) - rules" is then applied to the data. These rules select, classify and associate files on the basis of standardized FITS keywords that are present in the file header of the raw data and calibration data.

REFLEX workflows

The REFLEX workflow environment has been developed by ESO, to automate data reduction workflows. It provides a graphical user interface, with a flow-chart like representation of the steps required to perform data reduction. A REFLEX

workflow can be run with or without user interaction. The environment includes book keeping of data, a rule-based data organizer, and infrastructure to reuse results, among other user-friendly features. Concepts for early versions of REFLEX workflows for METIS currently exist for the imaging, longslit spectroscopy and integral field unit (IFU) observing modes. All workflows include the production of calibration frames, and the application of these master calibration frames to the science frames.

The imaging workflow additionally includes the calibration with standard stars. The longslit spectroscopy workflow also includes wavelength calibration, calibration with telluric standard stars and the application of an atmospheric model. The IFU workflow includes wavelength calibration, the application of an atmospheric model and a distortion model, rectification of spectra, and subsequent creation of an image cube with error maps.

3. TECHNICAL CONCEPT

3.1 Optical system

The optical overview of METIS is shown in Figure 5. The optical interface between the E-ELT and METIS is the telescope focal plane, which is located within volume allocated to LTAO (section 3.5). The interface between LTAO and METIS is 750mm downstream from the E-ELT focal plane. It is followed by the retractable feed mirror of the Warm Calibration Unit (WCU). Further downstream, 1000mm away from the E-ELT focal plane, the light enters the cryostat through the 230mm diameter ZnSe window that is slightly tilted (facing down) in order to avoid any contamination on the surface during operation. It is wedged to compensate for the dispersion introduced by the window itself and avoid Fabry-Perot fringing.

As can be seen in Figure 5 METIS has a modular concept. The central part is the common fore-optics (CFO) which "conditions" the beam and serves the various sub-systems (imager, IFS, AO WFS). The all-spherical CFO, shown in Figure 6, is responsible for reimaging the E-ELT focal plane (33″ field of view) inside the cryostat. In fact, the CFO is a double re-imager to accommodate all necessary functions: chopping, image de-rotation (or pupil co-rotation), cold calibration, thermal background and stray light reduction. The additional focal and pupil plane provided by the double relay CFO design make it possible to accommodate various high contrast imaging (HCI) modes as well. An extensive CFO trade-off study was done in order to find the optimal order of components and provide the best solution not only optically, but also from the perspective of science and operations. The co-rotating cold stop is located in the first pupil of the CFO, which is followed by the derotator, just in front of the first focal plane (FP1), positioned in gravity invariant (vertical) orientation. The subsequent AO pick-off mirror directs the near IR light (H, K bands) into the single conjugated adaptive optics (SCAO) subsystem. The second pupil of the CFO hosts a 2D-steerable beam "chopping" mirror [15], which switches between the target and a nearby reference sky (< 5 arcsec in any direction) for characterization of the temporally and spatially variable thermal background. Finally, the second focal plane of the CFO (FP2) contains a focal plane wheel with numerous field stops, slits, coronagraphic, and alignment masks. The CFO provides a focal plane for the science subsystems with an as-designed Strehl ratio of >0.99 at 2.9 μm over a FOV diameter of 23 arcsec (the full 33 arcsec input FOV is reduced by the ±5″ chopper throw). More information on the CFO can be found in [14].

The SCAO subsystem, which controls M4 and M5 of the E-ELT to apply the wavefront correction, is based on a Shack Hartmann wavefront sensor (WFS). A three lens achromat reimages the pupil plane, where the field selector is located. The latter is able to select the reference "star" anywhere within the 33″ FOV. Afterwards, in the proximity of the intermediate focal plane, a tip-tilt mirror is located that can be used to stabilize the pupil for the WFS. Finally, another achromatic triplet reimages the pupil onto the lenslet array. The SCAO is the only refractive optical system inside the METIS cryostat, consisting of BaF_2 and S-TIH53W lenses.

The second focal plane (FP2) of the CFO is the optical interface between the CFO and the science subsystems of the instrument. After FP2, a pick-off mirror reflects the light towards the LM band Spectrograph (LMS). When it is retracted, the full field of view is transmitted towards the LM and NQ band imagers (IMG). There is also a parallel observing mode, in which both the LMS and the LM IMG are used. In this case, the FOV surrounding the LMS pickoff is used by the imager, which implies that the science focal planes of these subsystems have to be coplanar.

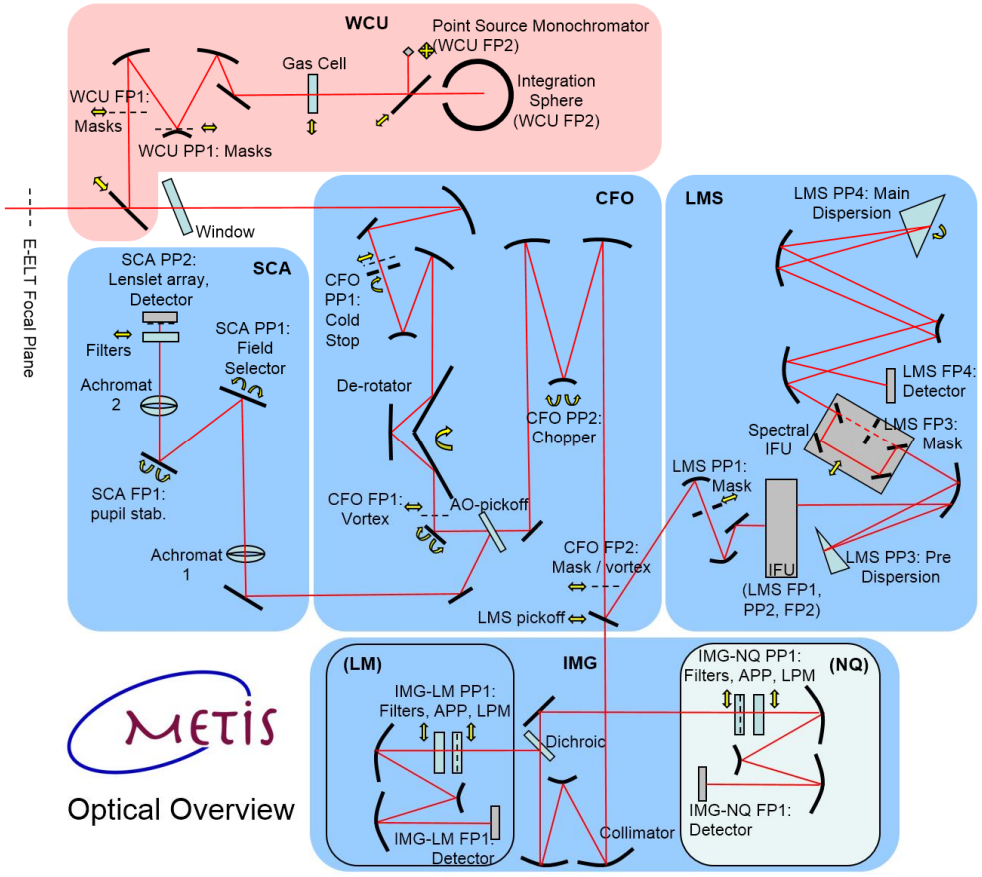

Figure 5 The optical system overview of METIS.

The high resolution (R=100,000 at 4.65μm) LMS is an integral field spectrometer, which operates in the 2.9-5.3μm wavelength range. After the LMS pickoff, the transfer optics reimages the focal plane onto the slicing mirrors of the Integral Field Unit (IFU), which reformats the image. The input FOV is slightly larger than 0.5″ × 0.5″, and the slice width is matched to λ/D at λ = 3.7μm, which corresponds to 0.0196″ on-sky. The pseudo-slit provided by the IFU is the input optical interface for the main optical unit of the LMS, which is based on an Echelle spectrometer. The main disperser is a silicon immersed grating [16] (section 3.6). An immersed grating demonstrator has been successfully built and its verification campaign just recently finished [17] (section 3.6). Regarding the optical design of the LMS, the immersed grating is positioned in a near-Littrow configuration inside a double pass three-mirror-anastigmat (TMA), and the necessary order separation is achieved by a ZnSe pre-disperser and a spatial filter. Extended wavelength coverage can be achieved by a 'spectral IFU' unit, which applies similar design principles as an IFU to provide an alternative to cross-dispersion [18].

The IMG provides diffraction limited imaging in a FOV of 11″×11″ at LM band and 15″×15″ at NQ band. Additionally, it provides coronagraphy and medium-resolution (1000 ≤ R ≤ 5000) long slit spectroscopy at LM and N bands. The optical system of the IMG uses a common TMA to collimate the beam, and subsequently a dichroic splits the light into the LM and NQ bands. Since the dichroic is upstream of the pupil, there is an accessible pupil in each imager arm, and various components, such as filters, coronagraphic masks and dispersers can be inserted in the beam via several pupil plane wheels. The LM and the NQ band cameras are also TMAs, which provide diffraction limited image quality at their specific wavelengths.

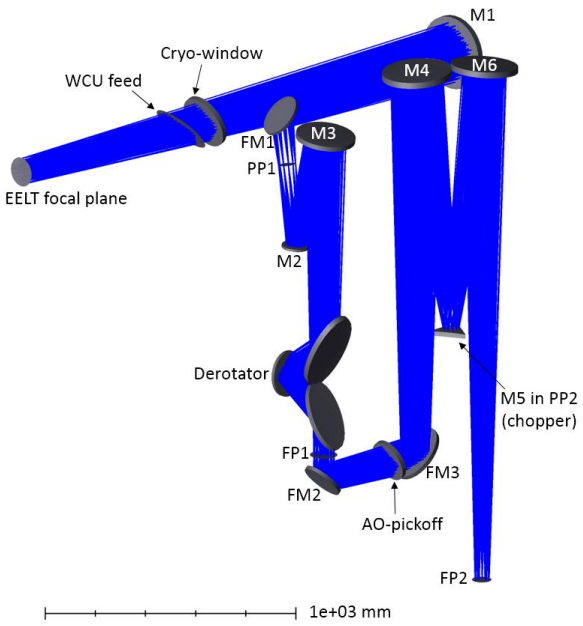

Figure 6 The optical design of the CFO. FP: focal plane, PP: pupil plane.

A sampling and FOV trade-off analysis has been performed, which showed that a slightly oversampled PSF is beneficial, and that the FWHM of the PSF at the shortest wavelength (3µm at LM and 8µm at NQ band) shall be distributed over three pixels. With a pixel scale of 18µm for the LM-band detector and 30µm for the NQ-band detector, the required camera f-ratios are 18 and 11.25, respectively. The IMG also contains a pupil imager, which is realized by inserting one ZnSe lens in front of the LM-band TMA and one behind it. The front-lens is mounted in one of the pupil wheels, while the rear lens is inserted and retracted via a dedicated mechanism.

The WCU is located above the cryostat. It enables the calibration of all scientific observing modes and can be used to monitor the stability of the instrument during daytime. Moreover, it will provide essential functionalities during AIV. The optical system of the WCU contains an Offner relay that is capable to reimage a series of selectable sources in the conjugate focal planes inside METIS: a diffraction-limited monochromatic point source, movable across the entire FOV, an extended source for flat fielding (covering the entire FOV) and a diffraction limited faint source for coronagraphy calibration (with a tunable distance from the main source). Additionally, a selection of gas cells can be inserted into the beam for calibration of the wavelength scale.

3.2 High contrast imaging

The most typical science case of METIS is that of imaging faint point and extended structures around stars, including extrasolar planets and debris disks. Hence, the performance in terms of high contrast imaging (HCI) is of utmost importance to METIS, including all aspects of imaging in the speckle-dominated domain, where the sky background limit is not reachable due to the diffraction halo of a bright, unresolved source.

METIS will have HCI observing modes for both imaging and spectroscopy. The HCI modes have small inner working angles (IWAs) to exploit the large aperture diameter of the E-ELT, and are implemented using three different sets of optics:

- *Focal plane coronagraphs*, which include variations based on the vortex coronagraph (VC). The vortex coronagraph concept is realized through annular groove phase masks (AGPMs). These are diamond optics etched via a spallation process to produce a series of annular concentric rings at a sub-wavelength spacing. The optics are 3mm thick with an etched diameter of 20mm, and are anti-reflection coated, optimized for the central wavelength of the band. The AGPM is placed in the focal plane of the telescope, and a star is placed on the central spot of the AGPM optic. A

second subsequent pupil plane uses a mask that blocks the star light scattered by the AGPM whilst allowing the circumstellar field to propagate with minimal attenuation. The VC is a high throughput coronagraph that provides 360 degrees of diffraction suppression around the central star, but its nulling depth is sensitive to residual vibrations from telescope and atmosphere that cannot be removed by the AO system, and to atmospheric dispersion at large zenith distances.

- *Pupil plane coronagraphs*, which are based on the apodizing phase plate (APP). The original design of the APP coronagraph uses variations in the thickness of a high refractive index material (for the thermal infrared, Zinc Selenide) to pattern variations in phase on a wavefront in the pupil plane. The resultant PSF in the focal plane shows the suppression of diffraction over a 180 degree field of view centered on the star. For METIS, a more recent manufacturing technique using liquid crystal polymers can produce APP patterns that are (i) very broadband, (ii) realise phase patterns that could not be manufactured with the earlier manufacturing techniques and (iii) be able to search in a 360 degree field of view around the star. These are called grating vector APPs (gvAPP). The APP coronagraph provides great performance with lower throughput than the best VC designs, but it is insensitive to telescope vibrations, allows beam switching at thermal infrared wavelengths, and is capable of dealing with the complex geometry of the telescope pupil. The IWA reaches down to 2λ/D and the throughput is lower than that of the ideal VC.
- *Interferometric imaging masks*, which provide high spatial resolution interferometry with sparse aperture masking (SAM) techniques. SAM is a single dish interferometric technique that masks out the majority of the telescope pupil to make a set of apertures with non-redundant pairs of baselines. These are pupil plane apertures that mask out the telescope pupil plane to leave a set of apertures whose pairwise combinations form a non-redundant set of baselines that form Young's fringes in the focal plane. Visibilities of the resultant fringes in the science camera focal plane can then be used to reconstruct the image of the source and can reach angular resolutions of 0.5λ/D, but with an attendant lower background sensitivity.

Coronagraphic configurations

A schematic overview of the light path in METIS along with the relevant pupil and focal plane locations for the HCI components is shown in Figure 7. Simulations by the METIS team showed that two coronagraphic configurations should be considered as baseline, namely the vAPP coronagraphs, and the vortex coronagraph combined with a Lyot phase mask (LPM), which provides good inner working angle performance.

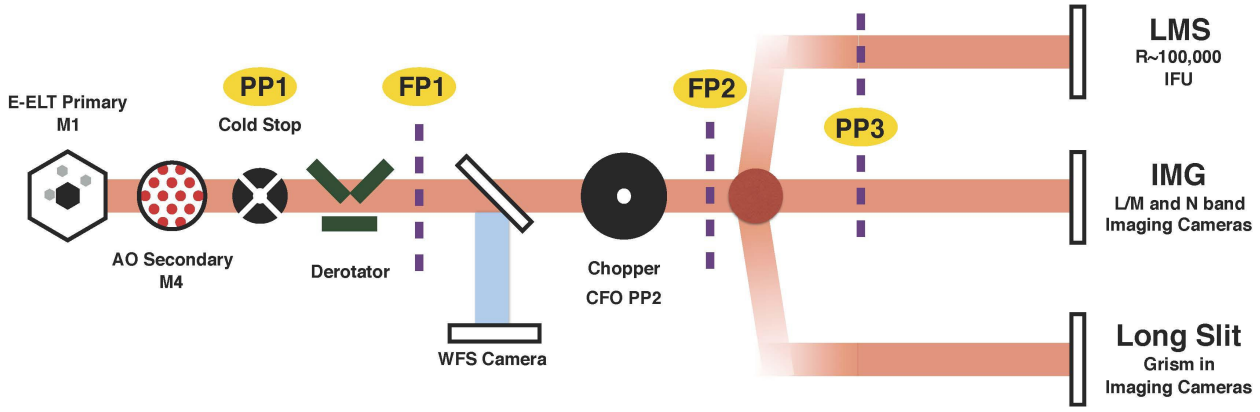

Figure 7 Schematic layout of the relevant optical components for HCI in METIS. The imaging cameras are represented as two separate paths labelled "Imaging Camera" and "Long Slit Spectrograph" to emphasize the different possible optical configurations. The accessible focal plane and pupil planes are labelled in a yellow ellipse.

Coronagraphy supported long-slit spectroscopy

The science case for METIS requires high contrast spectroscopy. However, the CFO and long slit configuration for the LM and NQ cameras cannot support coronagraphic imaging onto the slits at FP2, and the pupil position at PP2 is already occupied with the grism for the dispersion. The lack of a suitable focal plane and pupil plane before FP2 means that no focal plane coronagraph can be implemented for long slit spectroscopy. One proposed solution is a special vAPP optic

that has a bandpass capability that can transmit light shorter than 2.8μm to the WFS, but encode the APP phase pattern in light with wavelengths greater than 2.9μm to cover the L and M bands. This type of bandpass behavior is possible using liquid crystal deposition technology, and has been demonstrated for a filter in CRIRES on the VLT.

3.3 Adaptive optics

METIS will provide adaptive optics correction to enable stable high angular resolution required for its science observations. The classical single conjugate adaptive optics (SCAO) system is well suited for high contrast science cases, such as exoplanets and protoplanetary disks, which are observed in the vicinity of bright and compact on-axis reference objects. For the full scientific potential of METIS without the limitations on sky coverage that are inherent to SCAO a laser tomography adaptive optics (LTAO) system is considered as a future upgrade and must be included in the current conceptual design.

The SCAO WFS will be located inside the cryogenic environment of the instrument itself to minimize the thermal background introduced by the SCAO pickoff mirror. The SCAO loops will use the M4 and M5 mirrors of the E-ELT for wavefront correction. Besides the fast wavefront control loop, active non-common path aberration (NCPA) compensation will be implemented for high contrast imaging. Such an NCPA compensation will require the analysis of the science detector data in closed loop. In the optical path the SCAO pickoff mirror follows a common derotator and is relatively close to the science focal planes – this already reduces NCPA by design.

For the science cases that do not require high contrast imaging, the wavefront sensing reference target does not have to be on-axis but can be anywhere in the METIS FOV. In this case a field selection mirror inside the WFS will allow to select the reference target. The registration between M4 and the WFS will have to be controlled with a stabilization actuator.

METIS SCAO is expected to deliver a Strehl ratio of at least 93% at 10μm, and at least 60% at 3.7μm, on a 10 magnitude bright reference target under median seeing conditions. The results of the simulated AO performance as a function of seeing and brightness of the reference target are shown in Table 1. Furthermore, the performance of Pyramid and Shack-Hartmann (SH) wavefront sensor (WFS) types at visible and NIR wavelengths is also given in Table 1. The nominally better performance of the pyramid WFS on faint reference objects has to be balanced against the need for a complex cryogenic modulator. Because of its lower complexity a classical Shack-Hartmann near-infrared WFS option was chosen for the METIS SCAO design.

Sensor Type		Pyramid WFS				SH WFS											
Band		V		NIR		V						NIR					
Subaperture Diameter		0.5m	1.0m	0.5m	1.0m	0.5m			1.0m			0.5m			1.0m		
# Pix per Subaperture		2	2	2	2	2	4	6	2	4	6	2	4	6	2	4	6
Very bright good	SR@3μm	0.95	0.88	0.97	0.82	0.95	0.95	0.96	0.85	0.87	0.88	0.93	0.95	0.96	0.84	0.87	0.88
	Contrast@ 3λ/D x 10^4			0.19	0.18							0.16	0.42	0.43	0.18	0.32	0.35
Very bright median	SR@3μm	0.90	0.73	0.94	0.84	0.89	0.90	0.92	0.70	0.75	0.77	0.87	0.91	0.92	0.67	0.75	0.77
Very bright bad	SR@3μm	0.62	0.27	0.83	0.61	0.74	0.79	0.79	0.32[1]	0.52[1]	0.53	0.68	0.79	0.81	0.37[1]	0.49	0.51
Bright median	SR@3μm	0.90	0.72	0.94	0.83	0.88	0.90	0.91	0.69[1]	0.74	0.76	0.86	0.90	0.90	0.69[1]	0.74	0.75
Bright bad	SR@3μm	0.61	0.27	0.83	0.60	0.73	0.78	0.78	0.31[1]	0.50[1]	0.51	0.68	0.77	0.78	0.35[1]	0.47	0.49
Faint median	SR@3μm	0.90	0.70/0.65[3]	0.82	0.73	0.85	0.86	0.85	0.64[1]	0.63	0.61	0.70[2]	0.66	0.50	0.53	0.53	0.37
Faint bad	SR@3μm	0.59	0.26	0.67	0.44	0.66	0.64	0.66	0.22[1]	0.28[1]	0.30[1]	0.49[2]	0.45	0.35	0.22	0.24	0.19
Perf TT only	SR gain Res. jitter[mas]			0.15	0.14							0.47	0	0	0.82	0.19	0.03

Table 1: Simulated METIS SCAO performance.

3.4 Opto-mechanical system

The final performance of METIS depends strongly on the efficient minimization of instrumental thermal background radiation. Following Planck's radiation law required instrumental background temperatures for the L/M and N/Q band IM are around 80 and 30 Kelvin, respectively. For the infrared detector arrays, even lower temperatures of 40K and 8K for L/M and N/Q band, respectively, are required. To be able to cool METIS a stable vacuum environment is needed. The instrument is located in a dedicated cryostat, which consists of a protective shell with cooling systems, vacuum pumps, control systems, control software etc.

The cold optics bench within the cryostat is subdivided in various logical sub-systems, which will be designed, manufactured and tested as separate entities. This way a flexible instrument is created, where interfaces are defined such that maximum accuracy is gained with minimum effort, and additional interfaces can be identified for e.g. verification tools. Furthermore, concurrent engineering can take place on the various sub-systems, largely reducing total lead time of the instrument. A common cold central structure (CSS) acts as mechanical and thermal interface and provides the alignment of the modules with respect to each other and to the telescope image plane. Kinematic mounts are provided either to protect fragile optical components and/or to maintain accurate alignment and shape when cooling to operational temperatures.

The packaging is vital to locate the instrument properly within its allocated space envelope on the Nasmyth platform. An optical design using the minimum number of curved optical surfaces may extend beyond that envelope. By folding the optical system, the envelope can be used more efficiently. Locations of sub-systems can be steered toward areas with maximum envelope and easy access. Additional interfaces can be allocated for integration and verification purposes by allowing support equipment to be mounted at integrated locations. The overall packaging is dictated by the CFO, being the largest subsystem of METIS.

Considering the final size of METIS and the location of the focal plane with respect to the METIS mechanical interface on the Nasmyth platform, it is desirable to keep the centre of gravity as low as possible. This allows for a compact warm support structure (WSS) with minimum additional mass. The first Eigen-frequency of the system will increase, making the instrument less susceptible to base excitation via the platform. A more elongated shape allows for better accessibility to the cold optics bench in general, and especially providing sufficient envelope for the CSS for cooling lines and pads as well as stiffer design opportunities. More common cryostat base shapes can be used, like a cylinder with half spheres at its end. Figure 8 shows a proposed design with a preliminary packaging.

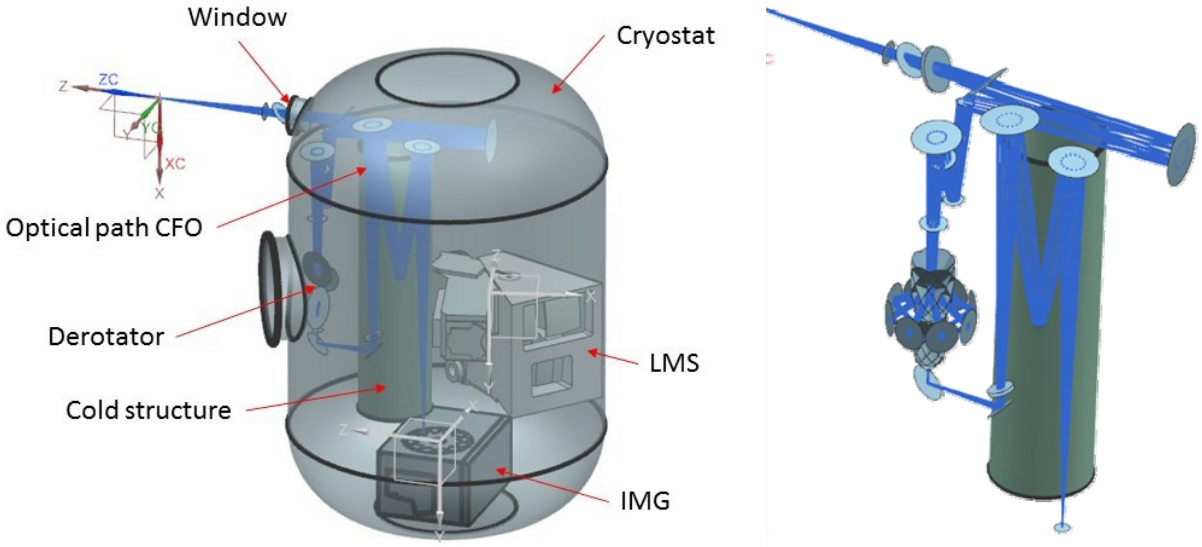

Figure 8 (Left) METIS cryostat showing the subsystems IMG and LMS ; not shown is the AO WFS. (Right) Zoom into the re-packaged CFO ; the symmetric structure near the center illustrates the various positions of the cryogenic derotator.

3.5 Telescope interface

Like the other two first-light instruments, HARMONI and MICADO, METIS will be located on the Nasmyth platform A of the E-ELT, see Figure 9. Light from the telescope is directed to the instruments on the lateral port with a retractable 90-degree folding mirror. That mirror is part of the so-called pre-focal station. The pre-focal station also takes care of the primary telescope guiding, active control of the internal telescope alignment, and co-phasing of the segments. The maximum field transmitted by the pre-focal station is 4.5 arcminutes in diameter for objects at infinity, and 2.6 arcminutes in diameter for the laser guide stars (LGS) at finite distance. Especially the latter yields a strong restriction on the available LGS configurations for METIS.

The optical axis is located at 6m height above the Nasmyth platform. METIS has stringent alignment requirements and with expected relative motions between the platform, METIS, and the pre-focal station, active control of the position is required to ensure a proper and stable alignment. With the current, compact design of the METIS cryostat, and space envelope allocated to the LTAO system (Figure 9), warm support structure (WSS) will be required to ensure that METIS and its LTAO system will not be impacted by platform motions and vibrations. The current mass budget for METIS is 9,000 kg, which, in light of the required support structure will be extremely challenging to achieve.

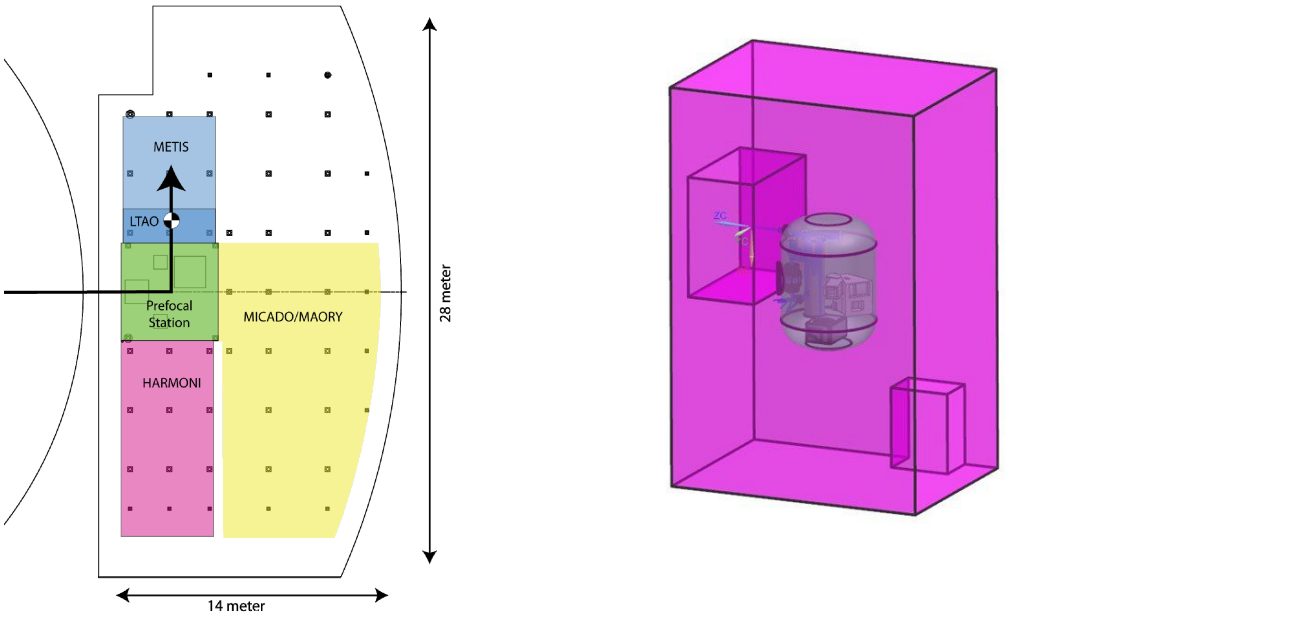

Figure 9. (Left) Provisional layout of the Nasmyth Platform A of the E-ELT. (Right) Location of the METIS cryostat within the volume allocated to METIS.

3.6 Immersed grating

METIS incorporates a couple of cryogenic key components, which have been previously developed for METIS. The cryogenic beam chopper [15] is one of them. Another one is the immersed grating for the LMS. In an immersed grating, the diffraction and interference occurs inside the silicon material which has a much higher refractive index than vacuum. It has several advantages, most importantly, the ability to decrease the size of the spectrograph and also excellent scattered light characteristics. With respect to a classical Echelle-type ruled grating, the optical path length and beam size can be significantly reduced.

The METIS immersed grating is based on a silicon prism, on one side with a bonded and fused silicon wafer in which the ruling profile has been etched with lithographic techniques. The METIS immersed grating measures 140mm × 80mm (dispersive vs. non-dispersive direction), enables R=100,000 at 4.65µm, and has a blaze angle of 55° and a groove density of 50 line pairs per millimeter.

In order to preserve the diffraction-limited image quality of METIS, the maximum RMS wavefront error (WFE) shall be less than 100nm. This WFE allocation comprises a large fraction of the total WFE budget of the entire spectrometer (153nm).

In order to prove the technology a research and development phase has been carried out, which culminated in the realization of a demonstrator, built at SRON/Utrecht and Philips Innovation Services, The Netherlands (Figure 10, left). Of particular importance was the study of the groove pattern, which has been made with conventional lithographic equipment, but the etching much deeper and the grating of much larger size than standard silicon parts for integrated circuits. Figure 10 (center) shows a SEM image of a test grating: the blaze angle is perfect and the surface extremely smooth, suppressing stray light.

However, tests of the demonstrator revealed that the WFE was significantly outside specifications. From a root cause analysis, and repeating the manufacturing steps, it was concluded that the increased WFE error resulted from a minimal variation in grating line position across the clear aperture. (The line position error must be less than 22nm RMS). The cause of the line position error could not be identified, but was likely due to a faulty step in the production chain. Remanufacturing of the wafer eventually delivered test wafers with acceptable line position errors Figure 10 (right) [17]. The next steps will include cryogenic cycling to study the bonding and behavior of bonding errors

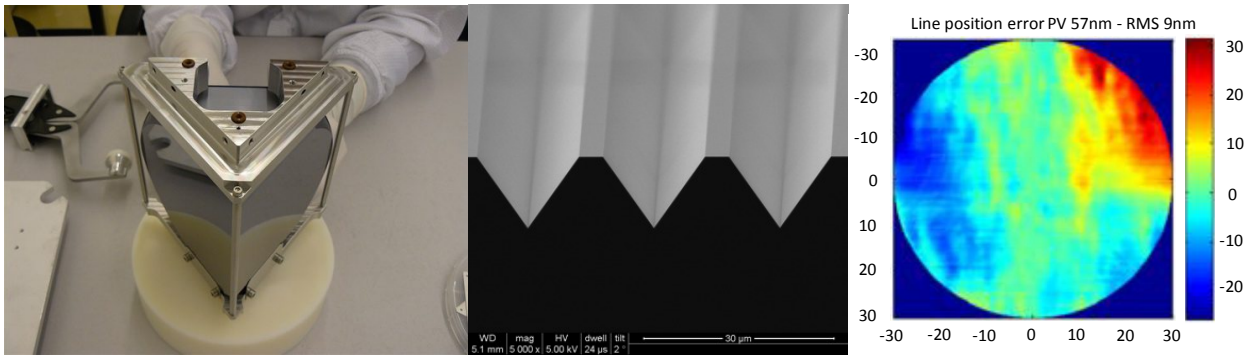

Figure 10 The METIS immersed grating. (Left) the assembled demonstrator. (Center) SEM image of a grating sample, showing the anisotropic (along the crystal boundary), etched grating pattern. (Right) Absolute line position error of the final test wafer measured inside the clear aperture. A peak-to-valley WFE of 57nm has been reached (RMS ~ 9nm), within specification.

3.7 Science focal plane detectors

The detector needs for METIS are relatively modest, in comparison to other E-ELT instruments. The baseline science detectors for the METIS imager are:

- one Teledyne 2k×2k HAWAII-2RG array, with a 5.3µm cutoff wavelength, for the L/M band IMG.
- one Raytheon 1k×1k AQUARIUS array for the N band IMG.
- four (2×2 array) Teledyne 2k×2k HAWAII-2RG arrays for the LMS. (The baseline has changed from the previous plan for a single 4k×4k device because of the availability of devices with 5.3µm cutoff wavelengths).

Mechanical mounts, electrical interfaces and cold preamplifiers already exist as the two types of detectors are in use within several ESO instruments (e.g., VISIR, HAWK-I). It is expected to reuse as much as possible the same designs for the detector interfaces with the instrument and the ESO environment.

One issue with the Aquarius detector is its excess low frequency noise (ELFN) which was noticed in the course of the upgrade of the VISIR instrument [20]. While the physics of this ELFN is understood (see references in [20]), the practical means of mitigation are limited. A detailed test campaign, led by the METIS detector team, will take place at ESO in summer of 2016. One possible measure is to increase the chopping frequency to reduce the amount of accumulated charges in each exposure. A more elegant but expensive solution would be the procurement of a new batch of ELFN-free Aquarius devices, which is currently under consideration.

REFERENCES

[1] Najita et al., ApJ, 589, 931 (2003)
[2] Pinilla et al., A&A 584A, 16P (2015)
[3] Pontoppidan et al., ApJ, 684, 1323 (2008)
[4] Brogi et al., Nature, Volume 486, 502 (2012)
[5] Snellen et al., Nature 509, 63S (2014)
[6] Borucki et al., ApJ 736, 19B (2011)
[7] Quanz et al., IJAsB 14, 279 (2015)
[8] Snellen et al., A&A 576, 59S (2015)
[9] Schmalzl, E., Meisner, J., Venema, L., Kendrew, S., Brandl, B., Blommaert, J., Glasse, A., Lenzen, R., Meyer, M., Molster, F., and Pantin, E., "An end-to-end instrument model for the proposed E-ELT instrument METIS," in [*Modeling, Systems Engineering, and Project Management for Astronomy V*], **8449**, 84491P (Sept. 2012).
[10] Ballester, P., Pizarro de La Iglesia, J. A., Modigliani, A., and Boitquin, O., "ETCs and Observations Simulation at the VLT," in [*Astronomical Data Analysis Software and Systems IX*], Manset, N., Veillet, C., and Crabtree, D., eds., *Astronomical Society of the Pacific Conference Series* **216**, 331 (2000).
[11] "New Method for Data Treatment Developed at ESO," in [*European Southern Observatory Press Release*], (Aug.1996). Available online at https://www.eso.org/public/news/eso9634/
[12] ESO CPL Development Team, "CPL: Common Pipeline Library", arXiv:1402.010 (2014)
[13] Freudling, W., Romaniello, M., Bramich, D.M., Ballester, P., Forchi, V., Garcia-Dablo, C.E., Moehler, S., Neeser, M.J., "Automated data reduction workflows for astronomy. The ESO Reflex environment", A&A, 559, A96 (2013)
[14] Agócs, T., et al., "Preliminary optical design for the common fore optics of METIS," Proc. SPIE 9908-360 (2016).
[15] Paalvast, S., Huisman, R., Brandl, B., Janssen, H., Jayawardhana, B., Molster, F., Teuwen, M., Venema, L., "Development and characterization of a 2D precision cryogenic chopper for METIS", Proc. SPIE 9151 (2014).
[16] van Amerongen, A.H., Agocs, T., van Brug, H., Nieuwland, G., Venema, L., Hoogeveen, R.W.M., "Development of silicon immersed grating for METIS on E-ELT", Proc. SPIE 8450 (2012).
[17] Agócs, T., et al., "Optical tests of the Si immersed grating demonstrator for METIS," Proc. SPIE 9912-41 (2016).
[18] Wells, M., et al., "Spectral slicing for METIS: an efficient alternative to cross-dispersion," Proc SPIE 9912-202 (2016).
[19] Kenworthy, M. A., Lacour, S., Kraus, A., Triaud, A. H. M. J., Mamajek, E. E., Scott, E. L., S´egransan, D., Ireland, M., Hambsch, F.-J., Reichart, D. E., Haislip, J. B., LaCluyze, A. P., Moore, J. P., and Frank, N. R., "Mass and period limits on the ringed companion transiting the young star J1407," MNRAS 446, 411–427 (Jan. 2015).
[20] Ives D., Finger G., Jakob G., Beckmann U., "Aquarius: the next generation mid-IR detector for ground based astronomy, an update", Proc. SPIE vol. 9154, 91541J (2014)